

Ultrasonic sensor based on phononic crystals

Paul Wasmer⁽¹⁾, Jannis Bulling⁽¹⁾, Jens Prager⁽¹⁾

⁽¹⁾Bundesanstalt für Materialforschung und -prüfung, Germany, paul.wasmer@bam.de

Abstract

An essential task in many industries, e.g. food, petrol or chemical industry, is the precise and accurate characterization of liquids. Therefore, the development of innovative in-line sensors is of great interest. New concepts based on periodic structures, so-called phononic crystals (PnCs), are an interesting idea for the design of new innovative sensors. A PnC-based sensor can be designed by introducing a resonance inside a bandgap, a frequency region where no wave propagation is allowed. High-Q measurement systems using PnCs are already reported in the literature. However, existing designs cannot be implemented into a piping system directly, but need special fittings, openings or by-passes to be in contact with the liquid. To circumvent this issue, we develop a new sensor based on PnCs, which can be directly implemented as part of the piping system. For this purpose, we use a PnC consisting of hollow cylinders with a periodic change of the outer diameter. A bandgap could be found for the described geometry without liquid in simulation and measurement. However, simulations show, that bandgaps for liquid-filled cylinders are very narrow, so that they cannot be used for the sensor design without additional effort. We therefore, propose a mode-selective excitation for the sensor design.

Keywords: Ultrasound, Phononic Crystals, Liquid Sensor

1 INTRODUCTION

The accurate and precise measurement of concentration of liquids is an essential task in many industries such as the petrol, the food, or the chemical industry. Measurement systems, which can easily be implemented into piping systems, are hereby of special interest. Besides other physical phenomena, ultrasonic waves can be used to determine liquid concentrations. New sensor concepts based on acoustic metamaterials, so-called phononic crystals (PnC's), are used to design ultrasonic measurement systems with high precision.

PnC's are periodic structures, which consists of at least two materials: a host matrix and periodically arranged scatterers inside the matrix. When an acoustic wave propagates through the crystal, it is scattered and due to the periodic arrangement of the scatterers destructive interference occurs. This leads to the formation of acoustic bandgaps, frequency regions in which no propagation of acoustic waves is allowed [1]. PnC's can be used for many different applications such as acoustic filtering [2], acoustic cloaking [3], waveguides [4] or sensor applications [5].

It is possible to design a PnC-based sensor to measure acoustic properties of a liquid. In the sensor design reported in the literature [6, 7, 8, 9], a defect in the crystal is used to create a resonance frequency in a bandgap. A resonance with a very small bandwidth is designed, which is sensitive to changes of the acoustic properties of the liquid. Inside the bandgap no wave propagates, but due to the defect the resonance frequency is enhanced and can propagate through the crystal. Due to the small bandwidth and the non-existence of other modes even small changes of the resonance frequency can be measured. Therefore, measurements with high quality can be obtained. By comparison to reference measurements, the acoustic properties and hence, the concentration of the liquid can be determined. In [8] it was shown that the ethanol concentration in gasoline can be determined using such a PnC-based sensor.

The described concept enables the investigation of very small liquid volumes without expensive hardware compared to time-of-flight approaches. Hence, the PnC-based sensors could be an interesting concept for microsensors [6]. Compared to other microsensors, such as Quartz Crystal Microbalance and Surface Acoustic Waves sensors, PnC-based sensors have the advantage, that the volumetric properties of the investigated liquid are measured, whereas the other principles often only measure surface properties [6]. PnC-based sensors are further of

interest for highly flammable or explosive liquids, as the electronic components can be easily separated from the liquid [8].

2 Tubular Bell

Existing PnC-based sensors show the great potential of this relatively new design [7, 8]. However, the existing sensors have a drawback: they are not very well suited to be used as an in-line sensor in a piping system. They cannot be implemented inside a piping system without additional fittings, windows or bypasses. To circumvent this issue Lucklum *et al.* [10] proposed a new PnC named “Tubular Bell“. The proposed PnC consists of an

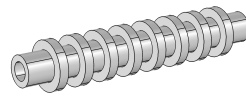


Figure 1. “Tubular Bell“ as proposed by Lucklum *et al.* [10].

array of hollow cylinders with a periodic change of the outer diameter (see Fig. 1). The proposed idea is to design a sensor with the “Tubular Bell“ based on the principle described in the previous section (Sec. 1). The PnC and hence the sensor can be designed as part of a piping system. The liquid flows through the constant inner diameter of the “Tubular Bell“. Therefore, additional fittings etc. can be omitted and no additional pressure loss occurs in the hydraulic system.

As the proposed sensor is based on PnC it is possible that the aforementioned advantages of the design (see Sec. 1) could be achieved as well.

To the best knowledge of the authors the proposed “Tubular Bell“ crystal is not yet described and investigated in the literature. Hence, before designing a sensor a detailed investigation of the acoustic behavior inside the “Tubular Bell“ is necessary.

2.1 Scaled boundary finite element method

Many simulations are needed to realize the “Tubular Bell“ sensor. Thus, a simulation method with high efficiency is essential. Therefore, the Scaled Boundary Finite Element Method (SBFEM) is used in this work. The SBFEM is a semi-analytical method, in which only the boundary of the computational domain is discretized with finite elements. The physical behavior inside the domain is described with an analytical ansatz. Therefore, the degrees of freedom of the numerical system are reduced and hence, shorter computational times can be realized compared to the classical Finite Element Method (FEM) [11]. This is especially of interest for simulation of ultrasonic waves. Due to the short wave length compared to the dimensions of the structure, large numerical systems have to be solved here.

For prismatic structures, such as cylinders, a special formulation of the SBFEM exists [12, 13]. This formulation is used for the SBFEM computations in this work. Hereby it is only necessary to discretize the base area of the cylinders, as displayed in Fig. 2. The wave propagation along the cylinder axis is described analytically.

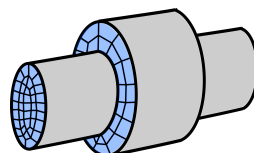


Figure 2. Discretized primitive cell of a “Tubular Bell“ PnC in the SBFEM.

2.2 Simulation

In contrast to the proposed “Tubular Bell“ hollow cylinder system, a periodic arrangement of full cylinders is investigated to begin with. This design was chosen due to the simpler manufacturing process.

Often PnC’s are only studied theoretically and not experimentally, hence not much information is available concerning the influence of the manufacturing process. Thus, this first study has also the goal to determine if manufacturing techniques, like lathing, achieve satisfactory results as geometrical variation influence the wave behavior.

2.3 Dispersion behavior

Bandgaps of PnC’s are determined by investigating the dispersion behavior in the crystals. In this work, all dispersion curves are computed via the commercial FEM-tool COMSOL Multiphysics®. For the computation of the dispersion curves, it is only necessary to simulate the primitive cell of the crystal, as the geometry outside repeats periodically.

As it convenient to reduce the computational time for simulations it is of interest to investigate how reduced,

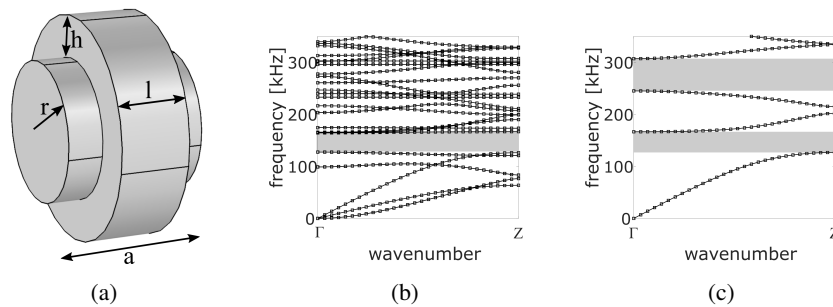


Figure 3. Dispersion curves of a crystal made from full cylinders; a) primitive cell b) dispersion curves for the 3D model c) dispersion curves for the axisymmetric model.

axisymmetric models compare to three-dimensional models. For this purpose we compute the dispersion behavior of both models. The investigated primitive cell is shown in Fig. 3a. The geometry parameters are given by: $r = 5$ mm, $h = 3$ mm, $l = 5$ mm and $a = 10$ mm. As material structural steel is used ($E = 200$ GPa, $\nu = 0.3$, $\rho = 7850$ kg m⁻³).

The results for the three-dimensional model are shown in Fig. 3b. A bandgap exists between 127 kHz and 164 kHz. A second bandgap does not appear in the investigated frequency domain.

The dispersion curves for the axisymmetric model are displayed in Fig. 3c. As expected the bandgap of the three-dimensional model is found in the same frequency region. Since most mode shapes (all bending modes and torsional modes) are neglected in the axisymmetric model, a second large bandgap (245 kHz – 307 kHz) occurs.

2.4 Transmission behavior

2.4.1 Simulation

The dispersion curves are computed for a perfect crystal; a crystal, with infinite length consisting of a periodic arrangement of primitive cells. Hence, it is possible that bandgaps only exist for crystals with large expansions or even just for the infinite structure. Therefore, it is necessary to investigate the transmission behavior of the crystal geometry with realistic, limited dimensions. For our investigation, we chose a crystal with eight repetitions of the primitive cell. The structure is excited with an equally distributed force on the base area of the first cylinder as shown in Fig. 4a. It is, therefore, an axisymmetric load. The amplitude of the force is constant over the investigated frequency range. As above, two simulation models are investigated: one three-dimensional model using COMSOL and an axisymmetric model using the SBFEM.

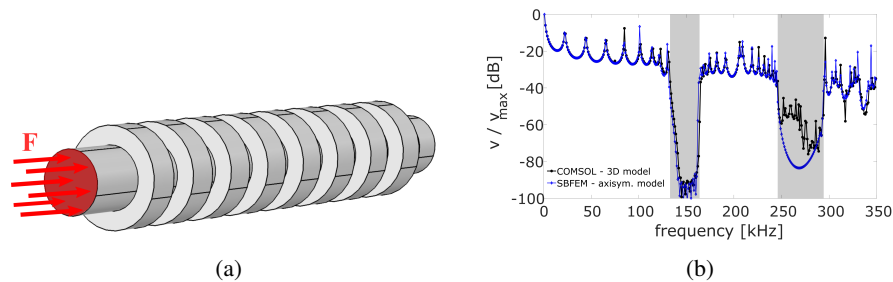


Figure 4. a) Simulation model of the PnC with an axisymmetric load b) Simulated transmission behavior of the investigated PnC.

The velocities in direction of the cylinder axis on the other end of the structure are investigated. In Fig. 4b the results are presented. The velocity for each frequency is related to the maximum of the occurring velocities. As expected, the results of both models are in very good agreement. In the axisymmetric, higher frequency bandgap, the models show the biggest difference. Compared to the axisymmetric model, the signal in the three-dimensional model has a larger, noisy amplitude. This might be related to the mesh, which is not perfectly axisymmetric. Other modes, which can propagate here, could be excited. The results show that an axisymmetric model can be used as a substituted in case of an axisymmetric load.

2.4.2 Measurement

The manufactured geometry is shown in Fig. 5a. On the end of the structure, a piezoelectric transducer is applied. It is a self-made transducer with a center frequency of 160kHz and a bandwidth of 54kHz. The transducer is excited using a sinus sweep from 50kHz to 350kHz. The signal is measured via a 3D laser vibrometer (Polytec PSV-500-3D-HV). The signal was measured on the base area of the cylinder and averaged

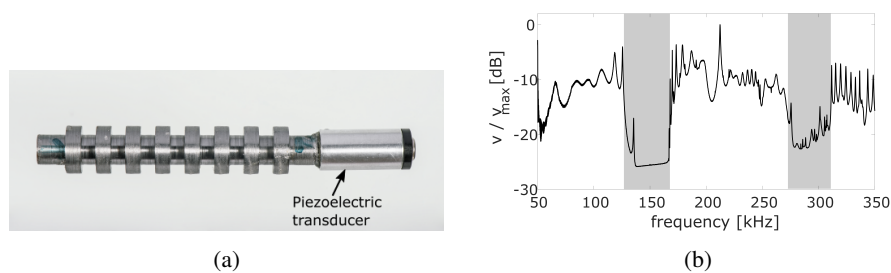


Figure 5. a) Manufactured PnC with applied transducer b) Transmission behavior of the investigated PnC.

over all measurement points. The measurement results are displayed in Fig. 5b. As before the displayed signal is related to the maximum of the measured velocities.

The first bandgap occurs in the expected frequency range (127kHz - 167kHz). At 135kHz one single mode is found inside the bandgap but as the signal is strongly reduced compared to the signal outside the bandgap it is not further investigated.

The purely axisymmetric bandgap cannot be determined with certainty, as not all modes are totally forbidden. A bandgap between 272kHz and 311kHz occurs. It is much smaller than in the simulation. As it is a purely axisymmetric bandgap, non-axisymmetric modes can propagate here. Therefore, the non-axisymmetric motion pattern of the piezoelectric transducer excites propagating modes.

The first bandgap of simulation and measurement are in very good agreement. The second bandgap cannot be

determined with certainty, which can be explained through the motion pattern of the transducer. Therefore, it can be concluded that tolerances of the manufacturing process were sufficiently small. Simulation, as well as measurements, suggest the sensor design should favor a bandgap, where the propagation of all modes is forbidden.

2.5 Resonance behavior

The sensor design is based on the resonance behavior of a defect. Therefore, it is of interest how a defect with resonance behavior can be introduced into the “Tubular Bell“. The studies are carried out without the liquid. Two variations of the “Tubular Bell“ are investigated: a crystal made out of full cylinders and a crystal made out of hollow cylinders. The crystal made out of full cylinders differs slightly from the already investigated version above (here $a = 9\text{mm}$) as to reduce the effect of the bandgap and gain a stronger signal inside the bandgap. The geometry parameters of the hollow cylinder crystal are given by (see Fig. 7a): $r = 5\text{mm}$, $r_i = 3\text{mm}$, $h = 3\text{mm}$, $l = 3\text{mm}$ and $a = 9\text{mm}$.

To introduce a resonance behavior the cylinder in the middle of the structure is varied in length and diameter. A resonance behavior is expected for a length of $\frac{\lambda}{2}$. But due to the complex wave behavior inside the crystal, the wavelength can only be estimated. In dispersive media, such as waveguides, the wavelength can be determined by investigating the dispersion behavior. However, inside the bandgap no wave propagation is possible and therefore no wavelength can be calculated for propagating waves.

2.5.1 Simulation

Axisymmetric SBFEM models are used for the simulation. The structures are excited as before with a constant force on one end. The signal is evaluated at the opposite end.

The length and the radius of the defect cylinder are varied until a resonance frequency is achieved inside the first bandgap. To realize a sharp resonance near the middle of the bandgap an optimization algorithm is applied. The restriction to the simulated frequencies is circumvented by fitting the results to a Lorentzian curve. The parameters of the fit (peak width, peak position, and peak height) are used for the objective function, which is minimized using a Nelder-Mead algorithm.

The resulted geometries and the related transfer functions are presented in Fig. 6. The different lengths and radii of the defect (see Fig. 6a and 6c) result from the optimization process.

The obtained resonance frequency of the defect for the full cylinder crystal is 148kHz. The transmission of the resonance frequency is still reduced compared to the signal outside of the bandgap. It has to be tested experimentally if the amplitude is large enough to be measured.

The resonance frequency of the hollow cylinder crystal is 114kHz. The signal at resonance frequency has as the signal outside of the bandgap. Hence, it should be reproducible in an experimental set-up.

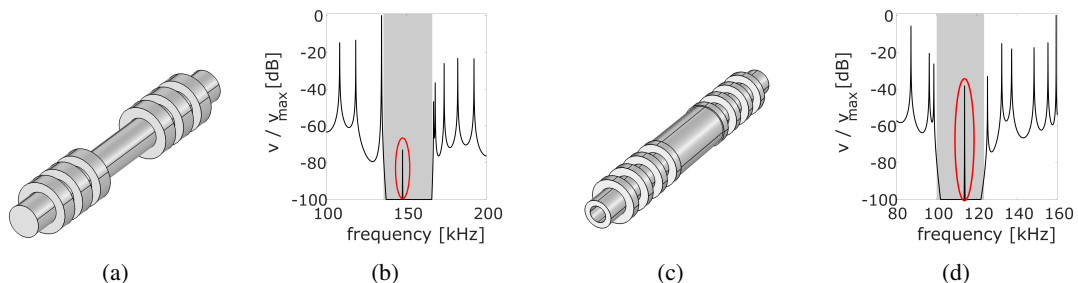


Figure 6. Optimized Geometries; a) full cylinder PnC b) transmission behavior of full cylinder PnC c) hollow cylinder PnC d) transmission behavior of hollow cylinder PnC.

A experimental validation of the experiments has yet to be made.

2.6 Sensor design

2.7 Dispersion behavior

All conducted studies so far neglect a liquid in the crystal. The basic design idea of a PnC sensor is to use a bandgap for the sensor development. Therefore, the dispersion behavior of a water-filled “Tubular Bell“ geometry (see Fig. 7a) is investigated. The same geometry parameters as in Sec. 2.5 are used.

The results are displayed in Fig. 7b for a 3D model. It can be seen that there exist only two very small bandgaps (97 kHz - 105 kHz and 130 kHz - 139 kHz) in the investigated frequency region. This can be explained through the occurring modes in both media. Inside the liquid exist only modes which are quasi-longitudinal. Therefore, there is no coupling (or only very weak coupling) between fluid modes and torsional or flexural modes of the solid. Hence, no large bandgaps occur.

In Fig. 7c the dispersion curves of an axisymmetric model are shown. Here, the same two bandgaps as in the

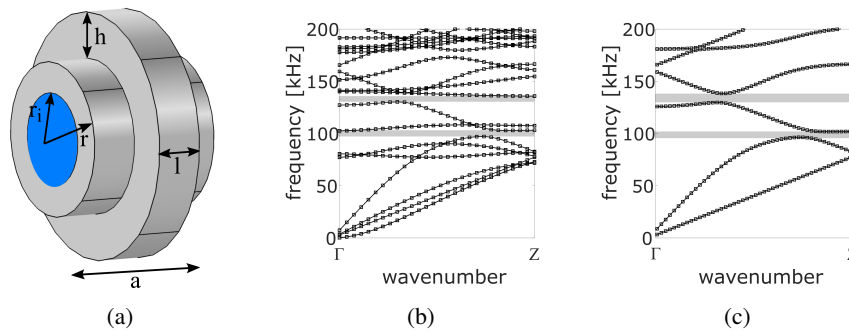


Figure 7. Dispersion for a water-filled “Tubular Bell“; a) primitive cell b) dispersion curves for a 3D model c) dispersion curver for a axisymmetric model.

3D model exist. However, both bandgaps are very small and are therefore not well suited to be used for the sensor development. It is a very challenging task to design a defect resonance in a very small bandgap. Thus, a mode-selective excitation could be used for the sensor design. In the region between both bandgaps only two modes exist. If those modes are not excited, no wave propagation occurs in this frequency region.

2.8 Transmission behavior with defect resonance

As there exist no large bandgap for a liquid-filled “Tubular Bell“, a mode-selective excitation can be used. For this purpose the region between the two bandgaps (97kHz - 139kHz) is selected. An excitation is chosen, which does not excite the two modes existing in this frequency region. This can be realized by an axisymmetric excitation on the outer diameter in direction of the cylinder axis.

The sensor is supposed to be part of a piping system. Therefore perfectly matched layers are used (marked in blue) at both ends to simulate the radiation into the pipe.

The transmission results for a crystal without defect are shown in Fig. 8a. A region without wave transmission exists between 87kHz and 116kHz. It matches not perfectly with the expected region but is sufficiently wide to be used for the sensor design.

By introducing a defect similar to the investigated models in Sec. 2.5 a resonance frequency can be found inside the region without wave transmission. The signal has to be measured near the defect as otherwise the amplitude is too small.

The investigated geometry (see Fig. 8b) has the potential to be used as a sensor. However, it has yet to be investigated, if this defect resonance is sufficiently sensitive to changes of the liquid properties. Furthermore, the peak of the resonance is still wide and needs be optimized towards a smaller bandwidth for the use in a

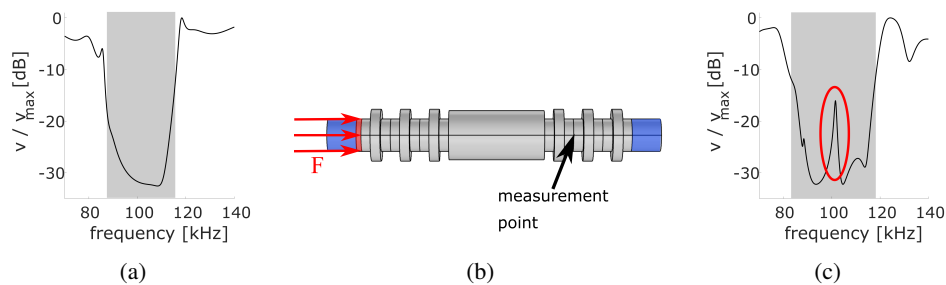


Figure 8. a) Transmission through the water-filled “Tubular Bell“ b) Simulation model with defect. The areas marked blue are the perfectly matched layers. c) Transmission through the water-filled “Tubular Bell“ with defect

sensor application.

3 Conclusion

PnC-based sensors are a promising new design idea for the measurement of liquid concentrations. A newly proposed design is the “Tubular Bell“; a PnC proposed for the purpose of an in-line sensor. The “Tubular Bell“ geometry was investigated in simulation and experiment, which both agree well. A resonance behavior with small bandwidth inside the bandgap could be realized for various geometries without liquid in simulations. The results have still to be confirmed in experiments.

In the liquid-filled crystal only small bandgaps occur. Therefore, a mode-selective excitation is needed. In simulations it could be shown that it is possible to have large frequency regions without wave propagation with an axisymmetric excitation on the outer diameter of the geometry. A defect can be used to achieve a resonance behavior. Further research is still necessary to show that the defect resonance can be used for sensor purposes.

REFERENCES

- [1] Kushwaha M. S., Halevi P., Dobrzynski L., Djafari-Rouhani B.: Acoustic band structure of periodic elastic composites. *Physical Review Letters* 71 (1993), pp. 2022 - 2025.
- [2] Pennec Y., Djafari-Rouhani B., Vasseur J., Khelif A., Deymier P.: Tunable filtering and demultiplexing in phononic crystals with hollow cylinders. *Physical Review E* 69 (2004), pp. 046608.
- [3] Zheng L.-Y., Wu Y. Ni X., Chen Z.-G., Lu M.-H., Chen Y.-F.: Acoustic cloaking by a near-zero-index phononic crystal. *Applied Physics Letters* 104 (2014), pp. 161904.
- [4] Vasseur J., Deymier P., Beaugeois M., Pennec Y., Djafari-Rouhani B., Prevost D.: Experimental observation of resonant filtering in a two-dimensional phononic crystal waveguide. *Zeitschrift für Kristallographie - Crystalline Materials* 220 (2009), pp. 829 - 835.
- [5] Nagaty A., Mehaney A., Aly A.: Acoustic Wave Sensor Based on Piezomagnetic Phononic Crystal. *Journal of Superconductivity and Novel Magnetism* 31 (2018), pp. 4173 - 4177.
- [6] Lucklum, R., Li, J.: - Phononic crystals for liquid sensor applications, *Measurement Science and Technology* 20 (2009), 124014 (12pp).
- [7] Villa-Arango, S., Torres, R., Kyriacou, P.A., Lucklum, R.: - Fully-disposable multilayered phononic crystal liquid sensor with symmetry reduction and a resonant cavity, *Measurement* 102 (2017), pp. 20 - 25.

- [8] Oseev, A., Zubtsov, M., Lucklum, R.: Gasoline properties determination with phononic crystal cavity sensor, *Sensor and Actuators B: Chemical* 189 (2013), pp. 208 - 212.
- [9] Oseeva A., Mukhina N., Lucklum R., Zubtsova M., Schmidt M.-P., Steinmann U., Fomind A., Kozyrevb A., Hirsch S.: Study of liquid resonances in solid-liquid composite periodic structures (phononic crystals) – theoretical investigations and practical application for in-line analysis of conventional petroleum products. *Sensors and Actuators B: Chemical* 257 (2018), pp. 469 - 477.
- [10] Lucklum, R., Zubtsov, M., Pennec Y.: Tubular Bell - New Class of (Bio)Chemical Microsensors. *Procedia Engineering* 120 (2015), pp. 520 - 523.
- [11] Wolf J.: *The scaled boundary finite-element method*, John Wiley & Sons, West Sussex, 2003.
- [12] Gravenkamp, H., Birk C., Song C. Simulation of elastic guided waves interacting with defects in arbitrarily long structures using the Scaled Boundary Finite Element Method, *Journal of Computational Physics* 295 (2015), pp. 438 - 455.
- [13] Krome F., Gravenkamp H., Birk C.: Prismatic semi-analytical elements for the simulation of linear elastic problems in structures with piecewise uniform cross section, *Computers and Structures* 192 (2017), pp. 83 - 95.
- [14] Gravenkamp H., Birk C., Song C.: The computation of dispersion relations for axisymmetric waveguides using the Scaled Boundary Finite Element Method, *Ultrasonics* 54 (2014), pp. 1737 - 1385.